

Random Currents Through Nerve Membranes

I. Uniform Poisson or White Noise Current in One-Dimensional Cables

Henry C. Tuckwell¹ and John B. Walsh²

¹ Department of Mathematics, Monash University, Clayton, Australia

² Department of Mathematics, University of British Columbia, Vancouver, Canada

Abstract. The linear cable equation with uniform Poisson or white noise input current is employed as a model for the voltage across the membrane of a one-dimensional nerve cylinder, which may sometimes represent the dendritic tree of a nerve cell. From the Green's function representation of the solutions, the mean, variance and covariance of the voltage are found. At large times, the voltage becomes asymptotically wide-sense stationary and we find the spectral density functions for various cable lengths and boundary conditions. For large frequencies the voltage exhibits " $1/f^{3/2}$ noise". Using the Fourier series representation of the voltage we study the moments of the firing times for the diffusion model with numerical techniques, employing a simplified threshold criterion. We also simulate the solution of the stochastic cable equation by two different methods in order to estimate the moments and density of the firing time.

1 Introduction

There are two neurophysiological situations with which we are concerned in this paper. In the first, the depolarization $V(x, t)$ of a nerve cylinder receiving synaptic excitation and inhibition (Rall, 1964) satisfies the equation

$$V_t = -V + V_{xx} + g_E[V_E - V] + g_I[V_I - V], \quad (1.1)$$

where V_E, V_I are constants, (providing very large ionic fluxes do not occur) called the excitatory and inhibitory reversal potentials, $g_E(x, t), g_I(x, t)$ are the corresponding conductances and subscripts t and x denote partial derivatives with respect to these variables. Usually $V_I < 0 < V_E$, so that when g_E is switched on, V increases (excitation), whereas when g_I is swit-

ched on V decreases (inhibition). Equation (1.1) is assumed to apply to single segments of neurons and in particular, portions of dendrites. Unfortunately it does not enjoy the property of mapping from dendritic trees to cylinders as does the usual cable equation under certain circumstances (Rall, 1962; Walsh and Tuckwell, 1983).

We are interested in the properties of V and other quantities associated with it when random synaptic conductance changes occur over the surface of the neuron. Examples of noisy voltage records from a cat spinal motoneuron are shown in Fig. 1A. The corresponding histogram of amplitudes and fitted Gaussian density are shown in Fig. 1B.

In the second situation of interest, the depolarization is governed by the Hodgkin-Huxley (1952) equations, the first of which is

$$V_t = V_{xx} + g_K[V_K - V] + g_{Na}[V_{Na} - V] + g_L[V_L - V], \quad (1.2)$$

where $g_K, g_{Na},$ and g_L are the potassium ion, sodium ion, and leakage conductances and $V_K, V_{Na},$ and V_L are the corresponding Nernst potentials. In the Hodgkin-Huxley system, g_K and g_{Na} are given in terms of other variables which satisfy further differential equations.

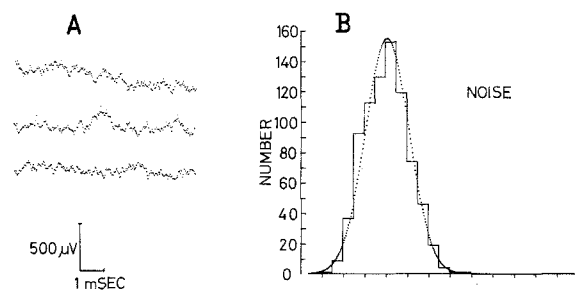


Fig. 1. A Voltage records from a resting spinal motoneuron. B Amplitude histogram of voltage noise and Gaussian density with the same mean and variance. The mean is zero and the voltage scale is marked at 50 μ V intervals. (From Jack et al., 1981)

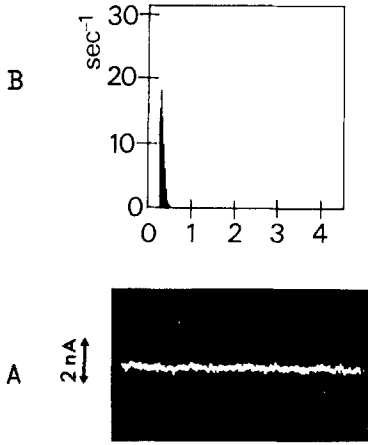


Fig. 2. A Current noise record from a squid axon. B Amplitude histogram (occurrences per second) of current noise; current in nA. (From Matsumoto and Shimizu, 1983)

Here we are interested in the properties of V when g_K and g_{Na} undergo random fluctuations due to the opening and closing of the corresponding ion channels. Examples of current noise records (Matsumoto and Shimizu, 1983) and the histogram of amplitudes for squid axon are shown in Fig. 2.

When g_E and g_I in Eq. (1.1) and when g_K and g_{Na} in Eq. (1.2) are random processes, the resulting equations are very difficult to study. As a first step in the direction of understanding their solutions we will consider the simpler cable equation,

$$V_t = -V + V_{xx} + r_m I, \quad a < x < b, \quad (1.3)$$

where $I(x, t)$ is a random (input) current density and r_m is the membrane resistance of unit length times unit length. For very small fluctuations in V from resting level, terms such as $V_E - V$ can be regarded as constants so that (1.3) provides a first approximation to (1.1) and (1.2). In fact (1.3) has been shown to be adequate for certain axons for depolarizations of many millivolts (Hodgkin and Rushton, 1946), and has often been employed in neural modeling (see e.g. Rall, 1977). Under certain geometrical conditions the potential over entire soma-dendritic surfaces can be found by solving (1.3).

In the model of the above phenomena that we consider, very short-lasting currents occur randomly along the length of the nerve cylinder. As a first approximation these may be treated as impulses so that the current density for a single occurrence at position x_i at time t_i is a multiple of $\delta(x - x_i)\delta(t - t_i)$. These impulses occur randomly at points of the semi-infinite strip $[a, b] \times R^+$ according to a Poisson point process which we can define as follows. Let $\lambda > 0$. For a

set $A \subset [a, b] \times R^+$, denote the number of impulses occurring in A by $\Pi^\lambda(A)$. Then:

(i) $\Pi^\lambda(A)$ is a Poisson random variable with parameter $\lambda|A|$, where $|A|$ is the Lebesgue measure (area) of A .

(ii) If A and B are disjoint, then $\Pi^\lambda(A)$ and $\Pi^\lambda(B)$ are independent. It will be useful note that

$$(iii) \text{Cov}[\Pi^\lambda(A), \Pi^\lambda(B)] = \lambda|A \cap B|.$$

We define a real-valued process $\{\Pi^\lambda(x, t), a \leq x \leq b, t \geq 0\}$ from this point process by $\Pi^\lambda(x, t) = \Pi^\lambda([a, x] \times (0, t])$. $\Pi^\lambda(x, t)$ is called the two-parameter Poisson process.

Since some currents are positive and others are negative, with various possible magnitude, we let V be governed by

$$V_t = -V + V_{xx} + \sum_i a_i \Pi_{xt}^{\lambda_i}, \quad a < x < b, \quad (1.4)$$

where $a_i, i = 1, 2, \dots$ are constants and $\Pi^{\lambda_i}, i = 1, 2, \dots$ are independent two-parameter Poisson processes with intensities λ_i . Note that

$$\begin{aligned} \Pi_{xt}^\lambda|_{(x_0, t_0)} &\doteq \frac{\partial^2 \Pi^\lambda}{\partial x \partial t} \Big|_{(x_0, t_0)} \\ &= \begin{cases} \delta(x - x_0)\delta(t - t_0), & \text{if there is a point at } (x_0, t_0) \\ 0, & \text{otherwise.} \end{cases} \end{aligned}$$

It is convenient for certain calculations to turn to a diffusion approximation (Walsh, 1981). Let $\{W(x, t) : a \leq x \leq b, t \geq 0\}$ be a Gaussian process defined as follows:

(i) $W(x, t)$ is a Gaussian random variable with mean zero and variance xt ;

(ii) $\text{Cov}[W(x, s), W(y, t)] = \min(x, y) \min(s, t)$.

Then W is called a standard two-parameter Wiener process or Brownian sheet. The stochastic equation for the diffusion model is formally written

$$\tilde{V}_t = -\tilde{V} + \tilde{V}_{xx} + \alpha + \beta W_{xt}, \quad a < x < b, \quad (1.5)$$

where α and β are constants. Note that $W_{xt} = \partial^2 W / \partial x \partial t$ is a white noise, and whilst the derivative does not exist in the usual sense, it is possible to make sense out of its integral,

$$W(x, t) = \int_a^x \int_0^t W_{ys} ds dy,$$

as in the one-parameter theory.

In the situations that concern us, there is good evidence that not much is lost in going from (1.4) to (1.5). If the impulses are very frequent and the charges delivered at each impulse are small, one expects the solution of (1.4) to be nearly continuous. Indeed, it was shown in Walsh (1981) that if the intensities λ_i increase

to infinity whilst the impulse sizes a_i decrease to zero in such a way that $\sum_i \lambda_i a_i \rightarrow \alpha$ and $\sum_i \lambda_i a_i^2 \rightarrow \beta^2$, then the solution of (1.4) tends to the solution of (1.5) in distribution.

To illustrate in a case where (1.1) applies, the total electrotonic length of the cylinder representing a cat spinal motoneuron is about 1.5 and the soma-dendritic surface is packed with about 20,000 synapses. About half of these are excitatory, the remainder being inhibitory (Conrad, 1969; Koziol and Tuckwell, 1978). When the mapping from dendritic tree to cylinder is performed, there will be several overlapping synaptic input sites at the same distance from the soma, especially at larger values of x .

As an example where (1.2) applies, Holden and Yoda (1981) estimate that there are about 200 sodium ion channels and about 100 potassium ion channels per square micron for squid axon. Using the standard data of 0.65 cm for the space constant and 500 microns for the diameter of a squid axon, there are about 2×10^9 sodium and 10^9 potassium channels per unit electrotonic length for this axon.

2 Solutions of the Stochastic Equations

The solution of Eq. (1.4) can be obtained formally using the impulse response function or Green's function, $G(x, y; t)$, which is the solution of the deterministic equation

$$G_t = -G + G_{xx}, \quad t > 0, \quad a < x < b, \quad (2.1)$$

with initial value

$$G(x, y; 0) = \delta(x - y), \quad a < y < b. \quad (2.2)$$

G satisfies the same (linear homogeneous) boundary conditions as those prescribed for $V(x, t)$ at $x = a$ and $x = b$. Nonhomogeneous boundary conditions, which are sometimes employed in the present context, can also be treated, but the formulas require slight modifications.

Assuming that V is initially zero on $a < x < b$, the solution of (1.4) is

$$V(x, t) = \sum_i a_i \int_a^b \int_0^t G(x, y; t-s) dI_i^2(s, y), \quad (2.3)$$

where the integrals are stochastic integrals with respect to Poisson processes in the plane. An outline of the theory and some properties of such integrals are contained in the appendix of Walsh (1981).

Accordingly, we have, for the mean depolarization,

$$E[V(x, t)] = \left(\sum_i \lambda_i a_i \right) \int_a^b \int_0^t G(x, y; t-s) ds dy. \quad (2.4)$$

The *covariance* of the depolarization at (x_1, t_1) and at (x_2, t_2) , with $t_2 \geq t_1 > 0$, is

$$\begin{aligned} K(x_1, t_1; x_2, t_2) &\doteq \text{Cov}[V(x_1, t_1), V(x_2, t_2)] \\ &= \left(\sum_i \lambda_i a_i^2 \right) \int_a^b \int_0^{t_1} G(x_1, y; t_1 - s) \\ &\quad \cdot G(x_2, y; t_2 - s) ds dy. \end{aligned} \quad (2.5)$$

This expression can be simplified by using the semi-group property of the Green's function:

$$\int_a^b G(x, z; s) G(y, z; t) dz = G(x, y; s+t).$$

Then (2.5) becomes

$$K(x_1, t_1; x_2, t_2) = \frac{1}{2} \left(\sum_i \lambda_i a_i^2 \right) \int_{t_2 - t_1}^{t_2 + t_1} G(x_1, x_2; s) ds, \quad (2.6)$$

The *variance* of $V(x, t)$ is $K(x, t; x, t)$.

The solution of Eq. (1.5) is

$$\begin{aligned} \tilde{V}(x, t) &= \alpha \int_a^b \int_0^t G(x, y; t-s) ds dy \\ &\quad + \beta \int_a^b \int_0^t G(x, y; t-s) dW(s, y), \end{aligned} \quad (2.7)$$

where the second integral is a stochastic integral with respect to the two-parameter Wiener process. It may be more intuitive to think of it as an integral with respect to white noise:

$$\int_a^b \int_0^t G(x, y; t-s) dW(s, y) = \int_a^b \int_0^t G(x, y; t-s) W_{ys} ds dy. \quad (2.8)$$

The theory of these stochastic integrals is outlined in the appendix of Walsh (1981). For our purposes the following facts are useful:

(i) $\int_a^b \int_0^t f(y, s) dW(y, s)$ is a Gaussian random variable with mean zero and variance $\int_a^b \int_0^t f^2(y, s) ds dy$;

$$\begin{aligned} \text{(ii) Cov} &\left[\int_a^b \int_0^{t_1} f(y, s) dW(y, s), \int_a^b \int_0^{t_2} g(y, s) dW(y, s) \right] \\ &= \int_a^b \int_0^{\min(t_1, t_2)} f(y, s) g(y, s) ds dy. \end{aligned}$$

It follows that the mean and covariance of \tilde{V} are given by (2.4) and (2.6) with the replacements

$$\alpha \leftrightarrow \sum_i \lambda_i a_i, \quad (2.9)$$

$$\beta \leftrightarrow \left(\sum_i \lambda_i a_i^2 \right)^{1/2}. \quad (2.10)$$

A Series Representation for \tilde{V}

It is useful to have a series representation for V for finite cables based on the Fourier series representation of the Green's function:

$$G(x, y; t) = \sum_n \phi_n(x) \phi_n(y) \exp[-\lambda_n t], \quad t > 0, \quad (2.11)$$

where $\{\phi_n\}$ is the set of normalized spatial eigenfunctions and $\{\lambda_n\}$ is the set of corresponding eigenvalues. Substituting (2.11) in (2.7) gives, with $a=0$, $b=L$,

$$\begin{aligned} \tilde{V}(x, t) = & \alpha \sum_n \phi_n(x) \int_0^L \int_0^t \phi_n(y) \exp[-\lambda_n(t-s)] dy ds \\ & + \beta \sum_n \phi_n(x) \int_0^L \int_0^t \phi_n(y) \exp[-\lambda_n(t-s)] dW(y, s). \end{aligned} \quad (2.12)$$

Define

$$\begin{aligned} V_n(t) = & \alpha \int_0^L \int_0^t \phi_n(y) \exp[-\lambda_n(t-s)] dy ds \\ & + \beta \int_0^L \int_0^t \phi_n(y) \exp[-\lambda_n(t-s)] dW(y, s), \end{aligned} \quad (2.13)$$

and

$$W_n(t) = \int_0^L \int_0^t \phi_n(y) dW(y, s). \quad (2.14)$$

Then, for fixed n , W_n is a standard one-parameter Wiener process, and, for different n , the processes W_n are independent (Walsh, 1981). Some careful manipulation will show that

$$\begin{aligned} V_n(t) = & \alpha \int_0^t \exp[-\lambda_n(t-s)] ds \\ & + \beta \int_0^t \exp[-\lambda_n(t-s)] dW_n(s), \end{aligned} \quad (2.15)$$

where

$$\alpha_n = \alpha \int_0^L \phi_n(y) dy. \quad (2.16)$$

Equation (4.5) shows that each V_n is an Ornstein-Uhlenbeck process with stochastic differential

$$dV_n = (\alpha_n - \lambda_n V_n) dt + \beta dW_n, \quad V_n(0) = 0. \quad (2.17)$$

For different n , the processes V_n are independent.

Thus the series (2.12) may be written

$$\tilde{V}(x, t) = \sum_n \phi_n(x) V_n(t). \quad (2.18)$$

Technical matters such as the convergence of this series were dealt with previously (Walsh, 1981). A similar series solution was employed in the study of the response of a nerve cylinder to white noise current injected at a point by Wan and Tuckwell (1979) and also in a study of the corresponding fitting time problem (Tuckwell et al., 1983).

3 Mean, Variance and Covariance of the Depolarization

In this section we will obtain expressions for the mean, variance and covariance for various cable lengths and boundary conditions. Since the formulas for \tilde{V} are obtained from those of V by the replacements (2.9) and (2.10), we will here use V to represent either V or \tilde{V} .

3.1 The Infinite Cable

For an infinite cable, the Green's function is

$$G(x, y; t) = \frac{\exp[-t - (x-y)^2/4t]}{\sqrt{4\pi t}}, \quad t > 0. \quad (3.1)$$

Using (3.1) in (2.4) gives

$$\begin{aligned} E[V(x, t)] = & \alpha \int_0^t \frac{\exp[-(t-s)]}{\sqrt{4\pi(t-s)}} \int_{-\infty}^{\infty} \\ & \cdot \exp[-\frac{1}{2}\{(y-z)/\sqrt{2(t-s)}\}^2] dy ds. \end{aligned} \quad (3.2)$$

The relation

$$\int_{-\infty}^{\infty} \exp[-z^2/2] dz = \sqrt{2\pi}, \quad (3.3)$$

is used to perform the y -integration; the subsequent s -integration gives the mean depolarization:

$$E[V(x, t)] = \alpha(1 - e^{-t}). \quad (3.4)$$

To obtain the covariance we use (3.1) in (2.6):

$$\begin{aligned} K(x_1, t_1; x_2, t_2) = & \frac{\beta^2}{4\sqrt{\pi}} \int_{t_2-t_1}^{t_2+t_1} \frac{\exp[-s - (x_1 - x_2)^2/4s] ds}{\sqrt{s}}. \end{aligned} \quad (3.5)$$

We utilize the relation

$$\begin{aligned} & \int_0^t \frac{\exp[-T - x^2/4T]}{\sqrt{T}} dT \\ & = \frac{\sqrt{\pi}}{2} \left[e^{-|x|} \operatorname{erfc}\left(\frac{|x| - 2t}{2\sqrt{t}}\right) - e^{|x|} \operatorname{erfc}\left(\frac{|x| + 2t}{2\sqrt{t}}\right) \right], \end{aligned} \quad (3.6)$$

where $\operatorname{erfc}(\cdot)$ is the complementary error function:

$$\operatorname{erfc}(x) = \frac{2}{\sqrt{\pi}} \int_x^{\infty} \exp[-z^2] dz. \quad (3.7)$$

This gives the required covariance,

$$\begin{aligned} K(x_1, t_1; x_2, t_2) = & \frac{\beta^2}{8} \left[e^{-|x_2 - x_1|} \left\{ \operatorname{erfc}\left(\frac{|x_2 - x_1| - 2(t_2 + t_1)}{2\sqrt{t_2 + t_1}}\right) \right. \right. \\ & \left. \left. - \operatorname{erfc}\left(\frac{|x_2 - x_1| - 2(t_2 - t_1)}{2\sqrt{t_2 - t_1}}\right) \right\} \right. \\ & \left. - e^{|x_2 - x_1|} \left\{ \operatorname{erfc}\left(\frac{|x_2 - x_1| + 2(t_2 + t_1)}{2\sqrt{t_2 + t_1}}\right) \right. \right. \\ & \left. \left. - \operatorname{erfc}\left(\frac{|x_2 - x_1| + 2(t_2 - t_1)}{2\sqrt{t_2 - t_1}}\right) \right\} \right]. \end{aligned} \quad (3.8)$$

There are several special cases of (3.8) which are of interest. The variance of $V(x, t)$ is

$$\operatorname{Var}[V(x, t)] = \frac{\beta^2}{4} [1 - \operatorname{erfc}(\sqrt{2t})]. \quad (3.9)$$

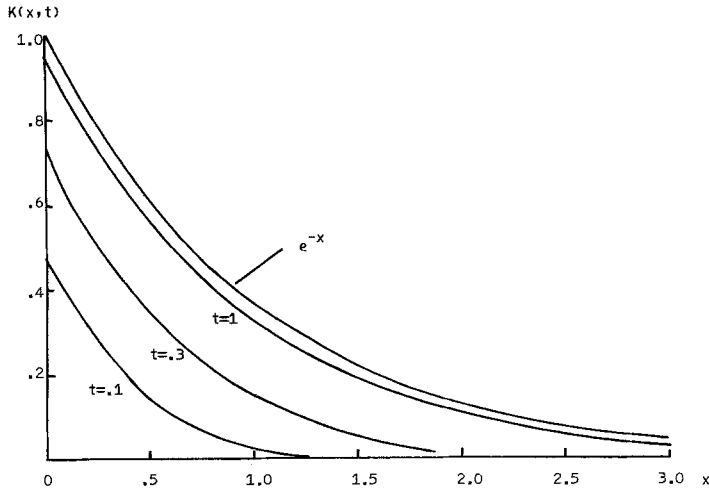


Fig. 3. Showing the approach of the covariance, $K(x, t_1; x, t_1 + \tau)$, of the voltage at a given space point to its asymptotic value for the infinite cable. ($\beta^2 = 4$)

Since $\text{erfc}(\infty) = 0$, in the steady-state $V(x, \infty)$ has mean α and variance $\beta^2/4$.

For $t_1 = t_2 = t$, the spatial covariance is $K(x_1, t; x_2, t)$

$$= \frac{\beta^2}{8} \left[e^{-|x_2 - x_1|} \text{erfc} \left(\frac{|x_2 - x_1| - 4t}{2\sqrt{2t}} \right) - e^{-|x_2 - x_1|} \text{erfc} \left(\frac{|x_2 - x_1| + 4t}{2\sqrt{2t}} \right) \right]. \quad (3.10)$$

Since $\text{erfc}(-\infty) = 2$, in the steady-state this becomes $\frac{\beta^2}{4} \exp[-|x_2 - x_1|]$. Note that for the diffusion model this implies, since V is Gaussian, that the depolarization becomes an Ornstein-Uhlenbeck process with x as parameter. Figure 3 shows the approach of the spatial covariance to its steady-state value.

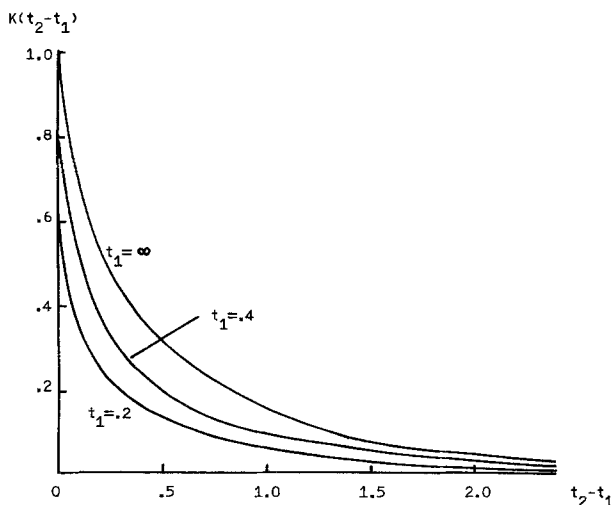


Fig. 4. Showing the approach of the spatial correlation of the voltage to its steady-state for the infinite cable. ($\beta^2 = 4$)

For $x_1 = x_2 = x$, the temporal covariance is found to be

$$K(x, t_1; x, t_2) = \frac{\beta^2}{4} [\text{erfc}(\sqrt{t_2 - t_1}) - \text{erfc}(\sqrt{t_2 + t_1})]. \quad (3.11)$$

This expression is plotted for various t_1 in Fig. 4.

When t_1 is large, put $t_2 = t_1 + \tau$. Then,

$$K(x, t_1; x, t_1 + \tau) \xrightarrow[t_1 \rightarrow \infty]{} \frac{\beta^2}{4} \text{erfc}(\sqrt{\tau}). \quad (3.12)$$

Hence, for large times the depolarization at a given space point becomes asymptotically wide-sense stationary (Doob, 1953). In fact, it can be seen that both V and \dot{V} become stationary as $t \rightarrow \infty$.

3.2 Finite Cables

Consider a finite cable on $0 \leq x \leq L$. We will concentrate on the following two sets of boundary conditions. Firstly, when *sealed ends* or short circuits terminate the cable at its end points,

$$V_x(0, t) = V_x(L, t) = 0. \quad (3.13)$$

Secondly, when the terminations are *killed ends* or open circuits, we have

$$V(0, t) = V(L, t) = 0. \quad (3.14)$$

In either case the Green's function, obtained by the method of separation of variables, can be expressed as in (2.11). For sealed ends the eigenvalues are

$$\lambda_n = 1 + n^2\pi^2/L^2, \quad n = 0, 1, \dots \quad (3.15)$$

and the normalized eigenfunctions are

$$\phi_n(x) = \begin{cases} 1/\sqrt{L}, & n = 0, \\ \sqrt{2/L} \cos(n\pi x/L), & n = 1, 2, \dots \end{cases} \quad (3.16)$$

In the case of killed ends, the eigenvalues are

$$\lambda_n = 1 + n^2\pi^2/L^2, \quad n=1, 2, \dots \quad (3.17)$$

and the normalized eigenfunctions are

$$\phi_n(x) = \sqrt{2/L} \sin(n\pi x/L), \quad n=1, 2, \dots \quad (3.18)$$

Substituting (2.11) in (2.4) gives, on performing the s -integration,

$$E[V(x, t)] = \alpha \sum_n \frac{\phi_n(x)}{\lambda_n} [1 - \exp(-\lambda_n t)] \int_0^L \phi_n(y) dy. \quad (3.19)$$

For sealed ends, therefore,

$$E[V(x, t)] = \alpha [1 - e^{-t}], \quad (3.20)$$

is the *mean* depolarization, with steady-state value α . For killed ends we obtain

$$E[V(x, t)] = \frac{4\alpha}{\pi} \sum_{n=1}^{\infty} \frac{\sin(n\pi x/L)}{n[1 + n^2\pi^2/L^2]} \cdot \{1 - \exp[-(1 + n^2\pi^2/L^2)t]\}, \quad (3.21)$$

where \sum' denotes summation over odd n only. The corresponding steady state value, which can be obtained by solving $-V'' + V = \alpha$, is

$$E[V(x, \infty)] = \alpha \left[1 + \frac{\sinh(x-L) - \sinh x}{\sinh L} \right]. \quad (3.22)$$

This function has a maximum value of $\alpha[1 - \operatorname{sech}(L/2)]$ at $x = L/2$.

To find the covariance we substitute (2.11) in (2.6) and, on performing the s -integration obtain the general expression,

$$K(x_1, t_1; x_2, t_2) = \beta^2 \sum_m \sum_n \phi_m(x_1) \phi_n(x_2) \cdot \exp[-(\lambda_m t_1 + \lambda_n t_2)] \cdot \int_0^L \phi_m(y) \phi_n(y) dy \int_0^{t_1} \exp[(\lambda_m + \lambda_n)s] ds. \quad (3.23)$$

When the spatial eigenfunctions are orthonormal, so that

$$\int_0^L \phi_m(y) \phi_n(y) dy = \delta_{mn}, \quad (3.24)$$

the double sum in (3.23) reduces to a single sum. On performing the s -integration we obtain the following general expression:

$$K(x_1, t_1; x_2, t_2) = \beta^2 \sum_n \frac{\phi_n(x_1) \phi_n(x_2)}{2\lambda_n} \cdot [\exp\{-\lambda_n(t_2 - t_1)\} - \exp\{-\lambda_n(t_2 + t_1)\}]. \quad (3.25)$$

Thus the variance of $V(x, t)$ is

$$\operatorname{Var}[V(x, t)] = \beta^2 \sum_n \frac{\phi_n^2(x)}{2\lambda_n} [1 - \exp\{-2\lambda_n t\}], \quad (3.26)$$

with steady-state value

$$\operatorname{Var}[V(x, \infty)] = \beta^2 \sum_n \frac{\phi_n^2(x)}{2\lambda_n}. \quad (3.27)$$

At $t_1 = t_2 = t$, the *spatial covariance* is

$$K(x_1, t; x_2, t) = \beta^2 \sum_n \frac{\phi_n(x_1) \phi_n(x_2)}{2\lambda_n} [1 - \exp\{-2\lambda_n t\}], \quad (3.28)$$

with steady-state value

$$K(x_1, \infty; x_2, \infty) = \beta^2 \sum_n \frac{\phi_n(x_1) \phi_n(x_2)}{2\lambda_n}. \quad (3.29)$$

For $x_1 = x_2 = x$, the *temporal covariance* is

$$K(x, t_1; x, t_2) = \beta^2 \sum_n \frac{\phi_n^2(x)}{2\lambda_n} \cdot [\exp\{-\lambda_n(t_2 - t_1)\} - \exp\{-\lambda_n(t_2 + t_1)\}]. \quad (3.30)$$

We put $t_2 = t_1 + \tau$ and find that

$$K(x, t_1; x, t_1 + \tau) \xrightarrow{t_1 \rightarrow \infty} \beta^2 \sum_n \frac{\phi_n^2(x)}{2\lambda_n} \exp\{-\lambda_n \tau\} \quad (3.31)$$

which shows that $V(x, t)$ for fixed x becomes asymptotically wide-sense stationary for large t .

To apply the above expressions for the covariance, one has to insert the eigenfunctions and eigenvalues appropriate for the given boundary conditions and, in most cases, evaluate the expressions numerically. Exceptions arise in that closed form expressions are obtained for the steady state variances and spatial covariances. These are found by applying the following formula (Gradshteyn and Ryzhik, 1966):

$$\sum_{k=1}^{\infty} \frac{\cos(kx)}{k^2 + \alpha^2} = \frac{\pi}{2\alpha} \frac{\cosh[\alpha(\pi - x)]}{\sinh(\alpha\pi)} - \frac{1}{2\alpha^2}. \quad (3.32)$$

Using this in (3.27) and (3.29) we find, for *sealed ends*, that the steady-state *variance* is

$$\operatorname{Var}[V(x, \infty)] = \frac{\beta^2 \cosh(L-x) \cosh x}{2 \sinh L}, \quad (3.33)$$

and the steady-state *spatial covariance* is,

$$K(x_1, \infty; x_2, \infty) = \frac{\beta^2 \cosh(L-x_1) \cosh x_2}{2 \sinh L}. \quad (3.34)$$

When the ends are *killed*, the steady-state *variance* is

$$\operatorname{Var}[V(x, \infty)] = \frac{\beta^2 \sinh(L-x) \sinh x}{2 \sinh L}, \quad (3.35)$$

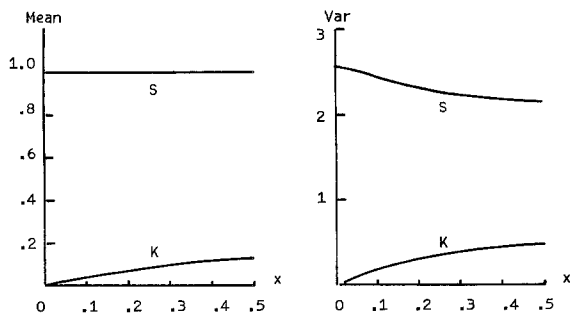


Fig. 5. Steady-state mean and variance of the voltage in the cases of S, sealed ends, and K, killed ends. ($L=\alpha=\beta=1$)

and the steady-state *spatial covariance* is,

$$K(x_1, \infty; x_2, \infty) = \frac{\beta^2 \sinh(L-x_1) \sinh x_2}{2 \sinh L}. \quad (3.36)$$

Notice that formulas corresponding to those obtained in this section can still be obtained when the spatial eigenfunctions are not orthogonal, as is the case, for example when the lumped soma termination is employed. In all cases, for physiological values of L , the approach to the steady-state is very rapid. Figure 5 shows the steady-state mean and variance of V for the cases of sealed and killed ends.

4 The Spectral Density of the Voltage

If $K(\tau)$ is the covariance kernel of a wide-sense stationary process, then the *spectral density function* of the process is defined as the Fourier transform,

$$f(\omega) = \frac{1}{2\pi} \int_{-\infty}^{\infty} \exp[-i\omega\tau] K(\tau) d\tau. \quad (4.1)$$

The spectral density is accessible experimentally and has been found for voltage and current noise in many neurophysiological preparations (see, for example, Finger and Stettmeier, 1980 and references therein).

In such experimentally determined spectral densities, the asymptotic behavior as $\omega \rightarrow \infty$ is often found to be $\sim k\omega^{-n}$, where k is a constant and $n \simeq 1$. This phenomenon has become generally called "1/f noise", and despite its ubiquity there does not appear to be a cogent theory (Hooge, 1976).

The processes we are concerned with contain two parameters, x and t , but we will examine the spectral density of the voltage at fixed x . We have seen that $V(x, t)$ and $\tilde{V}(x, t)$ become asymptotically stationary at large times. We assume, therefore, that sufficient time has elapsed since the beginning of the experiment to make the voltage at each point very nearly stationary so that we may meaningfully apply standard spectral analysis.

4.1 The Infinite Cable

Let the voltage be governed by either (1.4) or (1.5), with $-\infty < x < \infty$. At fixed x the covariance of $V(x, t_1)$ and $V(x, t_2)$ does not depend on x . We have found that

$$K(x, t_1; x, t_1 + \tau) \xrightarrow{t_1 \rightarrow \infty} \frac{\beta^2}{4} \operatorname{erfc}(\sqrt{\tau}),$$

which is only defined for $\tau \geq 0$. We omit all arguments except τ and extend K to negative values of τ in the natural way:

$$K(\tau) = \begin{cases} \frac{\beta^2}{4} \operatorname{erfc}(\sqrt{\tau}), & \tau \geq 0, \\ K(-\tau), & \tau < 0. \end{cases} \quad (4.2)$$

Since $K(\tau)$ is an even function of τ we have,

$$\begin{aligned} f(\omega) &= \frac{1}{\pi} \int_0^{\infty} \cos(\omega\tau) K(\tau) d\tau \\ &= \frac{\beta^2}{4\pi} \int_0^{\infty} \cos(\omega\tau) \operatorname{erfc}(\sqrt{\tau}) d\tau. \end{aligned} \quad (4.3)$$

Using the definition of $\operatorname{erfc}(\cdot)$,

$$f(\omega) = \frac{\beta^2}{2\pi^{3/2}} \int_0^{\infty} \cos(\omega\tau) \int_{\sqrt{\tau}}^{\infty} e^{-x^2} dx d\tau. \quad (4.4)$$

A consideration of the region of integration in the (x, τ) -plane yields:

$$\begin{aligned} f(\omega) &= \frac{\beta^2}{2\pi^{3/2}} \int_{x=0}^{x=\infty} e^{-x^2} \int_{\tau=0}^{\tau=x^2} \cos(\omega\tau) d\tau dx \\ &= \frac{\beta^2}{2\pi^{3/2}\omega} \int_0^{\infty} e^{-x^2} \sin(\omega x^2) dx. \end{aligned} \quad (4.5)$$

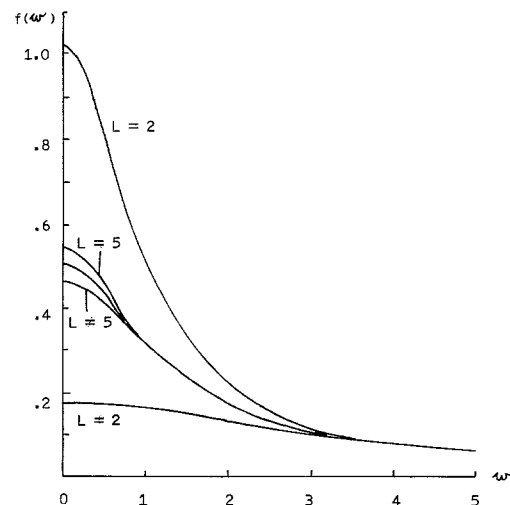


Fig. 6. Spectral density functions for various cable lengths and boundary conditions. The center curve is for the infinite cable; those above this curve are for sealed ends, those below for killed ends. Note the rapid approach to the asymptotic limit $\sim \omega^{-3/2}$. ($\beta^2 = 4\pi$)

This is a standard integral (Dwight, 1961) and we obtain the following expression for the *spectral density function of the voltage for an infinite cable with uniform white noise or Poisson input*:

$$f(\omega) = \frac{\beta^2}{4\pi} \frac{1}{\omega} \frac{\sin\left\{\frac{\arctan(\omega)}{2}\right\}}{(1+\omega^2)^{1/4}}. \quad (4.6)$$

This expression, with $\beta^2 = 4\pi$, is plotted in Fig. 6.

We have

$$f(0) = \beta^2/8\pi, \quad (4.7)$$

and asymptotically,

$$f(\omega) \underset{\omega \rightarrow \infty}{\sim} \frac{\beta^2 \sqrt{2}}{8\pi} \omega^{-3/2}. \quad (4.8)$$

Thus at high frequencies, the voltage noise on the infinite one-dimensional cable with uniform white noise or Poisson input exhibits “ $1/f^{3/2}$ noise”.

Notice that with our choice of units for time and the definition (4.1), the units of $f(\omega)$ are volts² per inverse time constant. If a time constant of 10 ms is assumed, then a frequency of 1000 Hz corresponds to $\omega = 20\pi$.

4.2 Finite Cables

Consider now solutions of (1.4) or (1.5) on $0 \leq x \leq L$. In the previous section we saw that at large times the solutions of the equations become, at fixed x , approximately covariance stationary, with kernel

$$K(\tau) = \frac{\beta^2}{2} \sum_n \frac{\phi_n^2(x)}{\lambda_n} \exp[-\lambda_n \tau], \quad \tau \geq 0. \quad (4.9)$$

$$f(\omega; L/2) = \frac{\beta^2}{4\pi\omega(1+\omega^2)^{1/2}} \left[\frac{\gamma \left(\frac{\sin(2L\varrho)}{2} \pm \cosh(L\gamma) \sin(L\varrho) \right) + \varrho \left(\frac{\sinh(2L\gamma)}{2} \pm \sinh(L\gamma) \cos(L\varrho) \right)}{\sinh^2(L\gamma) + \sin^2(L\varrho)} \right] \quad (4.17)$$

Again, we extend K to negative values of τ by putting $K(\tau) = K(-\tau)$, $\tau < 0$, so K is an even function of τ . For finite cables, the spectral density of $V(x, t)$ [or $\tilde{V}(x, t)$] depends on x . We make this dependence explicit and, on substituting (4.9) in (4.3) obtain

$$\begin{aligned} f(\omega; x) &= \frac{\beta^2}{2\pi} \sum_n \frac{\phi_n^2(x)}{\lambda_n} \int_0^\infty \cos(\omega\tau) \exp[-\lambda_n \tau] d\tau \\ &= \frac{\beta^2}{2\pi} \sum_n \frac{\phi_n^2(x)}{\lambda_n^2 + \omega^2}. \end{aligned} \quad (4.10)$$

We consider the two cases of sealed ends and killed ends.

For sealed ends, the eigenvalues are given by (3.15) and the eigenfunctions by (3.16). Therefore,

$$\begin{aligned} f(\omega; x) &= \frac{\beta^2}{2\pi L} \left[\frac{1}{1+\omega^2} + 2 \sum_{n=1}^\infty \frac{\cos^2(n\pi x/L)}{(1+n^2\pi^2/L^2)^2 + \omega^2} \right] \\ &= \frac{\beta^2}{2\pi L} \left[\frac{1}{1+\omega^2} + \frac{1}{i\omega} \sum_{n=1}^\infty \cos^2(n\pi x/L) \right. \\ &\quad \left. \cdot \left\{ \frac{1}{n^2\pi^2/L^2 + 1 - i\omega} - \frac{1}{n^2\pi^2/L^2 + 1 + i\omega} \right\} \right]. \end{aligned} \quad (4.11)$$

Using (3.32) this series may be summed, as in Walsh (1981) to give:

$$f(\omega; x) = \frac{\beta^2}{2\pi\omega} \mathfrak{I}_m \left\{ \frac{\cosh[(L-x)z] \cosh[xz]}{z \sinh[Lz]} \right\}, \quad (4.12)$$

where

$$z = \sqrt{1-i\omega} = (1+\omega^2)^{1/4} \exp\left[-\frac{i}{2} \arctan \omega\right], \quad (4.13)$$

and \mathfrak{I}_m denotes imaginary part. An expression in real variables is generally intractable. However, at the ends of the cable we find,

$$f(\omega; 0) = \frac{\beta^2}{4\pi\omega(1+\omega^2)^{1/2}} \left[\frac{\gamma \sin(2L\varrho) + \varrho \sinh(2L\gamma)}{\sinh^2(L\gamma) + \sin^2(L\varrho)} \right], \quad (4.14)$$

where

$$\gamma = (1+\omega^2)^{1/4} \cos\left\{\frac{\arctan \omega}{2}\right\}, \quad (4.15)$$

$$\varrho = (1+\omega^2)^{1/4} \sin\left\{\frac{\arctan \omega}{2}\right\}. \quad (4.16)$$

Similarly, at the center, we find

where the “+” refers to sealed ends and the “-” to killed ends.

Plots of f vs. ω at $x = L/2$ are given for various L and for sealed and killed ends in Fig. 3.

For killed ends, the eigenvalues are given by (3.17) and the eigenfunctions by (3.18). In this case the following general formula is obtained:

$$f(\omega; x) = \frac{\beta^2}{2\pi\omega} \mathfrak{I}_m \left\{ \frac{\sinh[(L-x)z] \sinh[xz]}{z \sinh[Lz]} \right\}. \quad (4.18)$$

The asymptotic behavior of (4.12) and (4.18), for $0 < x < L$, is the same as that for the spectral density in

the infinite cable case. In fact, it may be shown that for general linear homogeneous boundary conditions, the spectral density is

$$f(\omega; x) = \frac{\beta^2}{2\pi\omega} \int_0^\infty G(x, x; s) \sin(\omega s) ds, \quad (4.19)$$

and that the asymptotic behavior of the spectral density for large ω is always given by (4.8) at interior points of the interval of definition of V .

5 First Passage Times for the Diffusion Approximation

Whereas the cable equation applies in the first instance to nerve cylinders, it may, under certain conditions apply to neurons with dendritic trees (Rall, 1962; Walsh and Tuckwell, 1983). Points on the dendrites may be mapped onto a cylinder and the potential at those points mapped onto an "effective potential" which satisfies the cable equation on $(0, L)$, where L is the electronic distance from the origin or soma to the dendritic terminals. For details of the procedure and the conditions required for its validity, see Walsh and Tuckwell (1983).

If the neuron is subject to a uniform input current density over the dendrites, then, if certain geometrical constraints are satisfied, the effective potential V satisfies the cable equation with uniform input current density. Furthermore, the solution of this cable equation at $x=0$, is the potential at the soma.

We are concerned with a nerve cell which receives random synaptic bombardment over its dendritic surface. Assuming the stimulation is uniform we let the effective potential satisfy (1.4) on $(0, L)$. In this section we are concerned with the time between action potentials.

The cable equation has no natural threshold properties so that a threshold condition must be artificially imposed upon its solutions. If we endow the model neuron with a trigger zone or action potential generating region, located at the soma, then the simplest threshold condition is that a spike is generated when the somatic depolarization $V(0, t)$ reaches a constant threshold \mathfrak{g} .

We therefore define the random variable

$$T = \inf\{t | V(0, t) \geq \mathfrak{g}\}, \quad V(0, x) = 0, \quad 0 \leq x \leq L. \quad (5.1)$$

It should be borne in mind that this is not an accurate threshold criterion for many cells (Jack et al., 1975), but it will suffice here because we are interested only in general principles rather than a particular experimental situation. The techniques we apply may be used for various boundary conditions and threshold criteria.

First passage times for the case of Poisson input involve functional differential equations and are very difficult to handle. We will therefore focus on the diffusion approximation (1.5), with $0 \leq x \leq L < \infty$.

The Firing Time Problem

With the series representation (2.18) at our disposal we can make some progress with the determination of the time between spikes. Let the eigenvalues be $\lambda_1 < \lambda_2 < \dots$ with corresponding spatial eigenfunctions ϕ_1, ϕ_2, \dots and put

$$X_n(t) \doteq \phi_n(0)V_n(t) \quad (5.2)$$

with

$$X_n(0) = x_n. \quad (5.3)$$

Then from (2.17),

$$dX_n = [\bar{\alpha}_n - \lambda_n X_n] dt + \bar{\beta}_n dW_n, \quad (5.4)$$

where

$$\bar{\alpha}_n = \alpha_n \phi_n(0), \quad (5.5)$$

$$\bar{\beta}_n = \beta \phi_n(0). \quad (5.6)$$

The depolarization at the soma of the model neuron is

$$X(t) \doteq \sum_{n=1}^{\infty} X_n(t). \quad (5.7)$$

If one is interested in the threshold crossing at a point $x \neq 0$ then $\phi_n(x)$ will replace $\phi_n(0)$ in the above formulas.

Noting that X is continuous we define

$$T(\mathbf{x}) = \inf\left\{t | X(t) = \mathfrak{g} | X(0) = \sum_{n=1}^{\infty} x_n < \mathfrak{g}\right\}, \quad (5.8)$$

where $\mathbf{x} = (x_1, x_2, \dots)$. Then, for the model of firing that we are considering, the interspike time is

$$T = T(\mathbf{0}). \quad (5.9)$$

The m^{th} partial sum of the series (5.7) is

$$\bar{X}_m(t) = \sum_{n=1}^m X_n(t). \quad (5.10)$$

\bar{X}_m is also continuous so we put

$$T_m(\mathbf{x}_m) = \inf\left\{t | \bar{X}_m(t) = \mathfrak{g} | \bar{X}_m(0) = \sum_{n=1}^m x_n < \mathfrak{g}\right\}, \quad (5.11)$$

where $\mathbf{x}_m = (x_1, x_2, \dots, x_m)$. The approximate firing time based on approximating $X(t)$ with $\bar{X}_m(t)$ is $T_m(\mathbf{0})$.

The process X is an infinite-dimensional diffusion and the calculation of the statistical properties of its time $T(\mathbf{x})$ of first passage to \mathfrak{g} is not possible with presently known techniques. However, the process \bar{X}_m is an m -dimensional diffusion and first exit time theory for such processes is available (Dynkin, 1965).

To utilize this theory we note that the infinitesimal generator of the vector-valued diffusion $\bar{\mathbf{X}}_m = (X_1, X_2, \dots, X_m)$ is

$$\frac{1}{2} \sum_{n=1}^m \beta_n^2 \frac{\partial^2}{\partial x_n^2} + \sum_{n=1}^m (\bar{\alpha}_n - \lambda_n x_n) \frac{\partial}{\partial x_n} \doteq \mathcal{L}_{\mathbf{x}_m}. \quad (5.12)$$

First passage of $\bar{\mathbf{X}}_m(t)$ to \mathcal{G} occurs when the vector $\bar{\mathbf{X}}_m(t)$ first exits from the half-space $\sum_{n=1}^m x_n < \mathcal{G}$. It is established (Walsh, 1981) that this first exit time is finite with probability one and has finite moments of all orders. Thus, if the k^{th} moment of $T_m(\mathbf{x}_m)$ is denoted by $\mu_{m,k}(\mathbf{x}_m)$, we have (Dynkin, 1965),

$$\begin{aligned} \mathcal{L}_{\mathbf{x}_m} \mu_{m,k}(\mathbf{x}_m) &= -k \mu_{m,k-1}(\mathbf{x}_m), \\ k &= 1, 2, \dots, \mu_{m,0} = 1 \end{aligned} \quad (5.13)$$

with $\mu_{m,k}$ vanishing on the hyperplane $\sum_{n=1}^m x_n = \mathcal{G}$. The partial differential equations (5.13) may be solved numerically for various k and m to obtain estimates of the moments of the firing time.

Note that a crude estimate of the firing time for a general threshold function may be found. Let \tilde{V} be the weak solution of (1.5) with sealed-end conditions at $x=0$ and $x=L$. Define

$$T_{\mathcal{G}} = \inf \left\{ t \mid \sup_x (\tilde{V}(x, t) - \mathcal{G}(x)) \geq 0 \mid \tilde{V}(x, 0) = 0 \right\},$$

and assume that the threshold function \mathcal{G} has the Fourier expansion

$$\mathcal{G}(x) = \sum_{n=1}^{\infty} a_n \phi_n(x),$$

where $\phi_1 = L^{-1/2}$, $\phi_n = (2/L)^{1/2} \cos(n\pi x/L)$, $n=2, 3, \dots$. Put

$$\tilde{V} = \sum_{n=1}^{\infty} Y_n$$

where

$$Y_n = \phi_n(x) V_n(t).$$

Let

$$T_1 = \inf \{ t \mid Y_1(t) \geq a_1 \phi_1 \mid Y_1(0) = 0 \}.$$

Then

$$T_{\mathcal{G}} \leq T_1.$$

To see this, note that

$$T_{\mathcal{G}} = \inf \left\{ t \mid \sup_x \left(\sum_{n=1}^{\infty} (V_n(t) - a_n \phi_n(x)) \right) \geq 0 \mid \tilde{V}(x, 0) = 0 \right\}.$$

But with the given boundary conditions

$$Y_1(t) - a_1 \phi_1 = \frac{1}{L} \int_0^L (\tilde{V}(x, t) - \mathcal{G}(x)) dx.$$

Hence, whenever $Y_1 \geq a_1 \phi_1$ the integral on the right is positive, which implies that $V(x, t) \geq \mathcal{G}(x)$ for some x . Thus, $T_{\mathcal{G}} \leq T_1$.

This estimate is useful because T_1 is the first passage time of an Ornstein-Uhlenbeck process to a constant level. Calculations of the moments of T_1 have been performed (Wan and Tuckwell, 1982 and references therein).

Examples of Numerical Calculation of the Mean Firing Time

In the following we assume that there are sealed ends at $x=0$ and $x=L$. Other boundary conditions may be treated in the same way with allowance for different eigenvalues and eigenfunctions. In the present case the eigenvalues are given by (3.16) and the eigenfunctions by (3.15). The Eq. (5.4) are then

$$dX_1 = (\alpha - X_1)dt + (\beta/\sqrt{L})dW_1, \quad (5.14)$$

$$dX_n = -\lambda_n X_n dt + \beta \sqrt{2/L} dW_n, \quad n=2, 3, \dots \quad (5.15)$$

In the following numerical work we consider the calculation of the mean firing time for the two-component approximation $\bar{\mathbf{X}}_2 = X_1 + X_2$. The differential equation for the mean firing time is

$$\begin{aligned} \frac{\beta^2}{2L} \left[\frac{\partial^2 \mu_{2,1}}{\partial x_1^2} + \frac{2\partial^2 \mu_{2,1}}{\partial x_2^2} \right] + (\alpha - x_1) \frac{\partial \mu_{2,1}}{\partial x_1} \\ - (1 + \pi^2/L^2) x_2 \frac{\partial \mu_{2,1}}{\partial x_2} = -1. \end{aligned} \quad (5.16)$$

We are mainly interested in the value of the solution of this equation at $x_1 = x_2 = 0$. Therefore, in a numerical solution we consider (5.16) on a finite rectangle with one side along $x_1 + x_2 = \mathcal{G}$ and which contains $(0, 0)$.

Simulation Methods

The use of numerical methods for solving the partial, differential equations (5.13) is usually inefficient because:

(i) to find the solution at one point one has to generate the solution at several points in a large region surrounding that point;

(ii) to solve the equation for the second moment of the firing time one needs a solution of the equation for the first moment whose accuracy exceeds that required for the second moment;

(iii) to find the density, $p(\mathbf{x}_m, t)$ of the first exit time of the m -dimensional diffusion $\bar{\mathbf{X}}_m$, one has to solve the $(m+1)$ -dimensional partial differential equation,

$$\mathcal{L}_{\mathbf{x}_m} p(\mathbf{x}_m, t) = \frac{\partial p}{\partial t}. \quad (5.17)$$

Hence, even with just two terms in the series one has to solve a three-dimensional equation.

It is therefore desirable to use simulation methods which can yield estimates of the moments and density of the firing time. We have investigated two simulation methods, which we now describe.

Simulation of the Series $\bar{X}_m(t)$

Approximate sample paths for $\bar{X}_m(t)$ may be generated as follows. First we write out the integral representations of the terms in the series:

$$X_1(t) = \alpha(1 - e^{-t}) + \frac{\beta}{\sqrt{L}} e^{-t} \int_0^t e^s dW_1(s), \quad (5.18)$$

$$X_n(t) = \beta \sqrt{\frac{2}{L}} e^{-\lambda_n t} \int_0^t e^{\lambda_n s} dW_n(s), \quad n=2, 3, \dots, \quad (5.19)$$

where it has been assumed that $X_n(0) = 0$, $n=1, 2, \dots$. The (Ito) stochastic integrals in (5.18) and (5.19) are limits in mean square, as $\Delta s \rightarrow 0$, $M \rightarrow \infty$, with $t = M\Delta s$, of random sums. Hence we put,

$$\begin{aligned} \tilde{X}_1(t) &\doteq \alpha(1 - e^{-t}) + e^{-t} \frac{\beta}{\sqrt{L}} \sum_{k=1}^M \exp[(k-1)\Delta s] \\ &\cdot \{W_1(k\Delta s) - W_1((k-1)\Delta s)\}, \end{aligned} \quad (5.20)$$

$$\begin{aligned} \tilde{X}_n(t) &\doteq \beta \sqrt{\frac{2}{L}} \exp[-\lambda_n t] \sum_{k=1}^M \exp[\lambda_n(k-1)\Delta s] \\ &\cdot \{W_n(k\Delta s) - W_n((k-1)\Delta s)\}, \quad n=2, 3, \dots \end{aligned} \quad (5.21)$$

For large M , (5.20) and (5.21) may be used to approximate (5.18) and (5.19). In the actual simulations, the increments in the Wiener processes are replaced by random samples of normal random variables with the correct variances. Thus, let $N_{n,k}$, $n=1, 2, \dots$; $k=1, 2, \dots$ be families of independent standard normal random variables. Then the simulations are performed by replacing (5.20) and (5.21) by,

$$\begin{aligned} \tilde{X}_1(t) &= \alpha(1 - e^{-t}) + e^{-t} \frac{\beta}{\sqrt{L}} \sqrt{\Delta s} \sum_{k=1}^M \\ &\cdot \exp[(k-1)\Delta s] N_{1,k}, \end{aligned} \quad (5.22)$$

$$\begin{aligned} \tilde{X}_n(t) &= \beta \sqrt{\frac{2}{L}} \exp[-\lambda_n t] \sqrt{\Delta s} \sum_{k=1}^M \\ &\cdot \exp[\lambda_n(k-1)\Delta s] N_{n,k}, \quad n=2, 3, \dots \end{aligned} \quad (5.23)$$

We compute the values of \tilde{X}_1, \tilde{X}_2 , etc. for $M=1, 2, \dots$ and the corresponding values of their sum

$$\tilde{X}_m = \sum_{n=1}^m \tilde{X}_n(t), \quad (5.24)$$

and record the time at which \tilde{X}_m first reaches or exceeds \mathfrak{A} . This is done for N trials, whereupon sample mean, sample standard deviation and histogram of the firing time can be found.

Simulation of the Stochastic Integral Solution

At small t (less than about 0.2 for typical values of L), the convergence of the eigenfunction expansion (2.11) for the Green's function is very slow. At such values of t , the first few terms of the series (5.7) are an inadequate approximation to $\tilde{V}(x, t)$. If the interspike interval density is concentrated appreciably at such values of t , then the values of the interspike time obtained by the simulation of the first few terms of the Fourier series are not a reasonable approximation to the actual interspike time.

It is therefore sometimes advantageous to simulate $\tilde{V}(x, t)$ by appealing directly to its definition through the stochastic integral in (2.7). Let \tilde{V}_R be the random component of \tilde{V} :

$$\tilde{V}_R(x, t) = \beta \int_0^t \int_0^L G(x, y; t-s) dW(s, y). \quad (5.25)$$

By definition of stochastic integral we have,

$$\begin{aligned} \tilde{V}_R(x, t) &= \beta \lim_{\substack{m \rightarrow \infty \\ n \rightarrow \infty}} \sum_{i=1}^m \sum_{j=1}^n \\ &\cdot G(x, i\Delta y; (n-j+1)\Delta s) W(\Delta A_{ij}), \end{aligned} \quad (5.26)$$

where \lim means limit in mean square, $\Delta y = L/m$, $\Delta s = t/n$ and ΔA_{ij} is the rectangle

$$[i\Delta y, (i+1)\Delta y] \times [j\Delta s, (j+1)\Delta s].$$

Since $W(\Delta A_{ij})$ is normal with mean zero and variance $\Delta s \Delta y$, an approximate discrete realization of \tilde{V}_R is afforded by setting, with Δs and Δx "small",

$$\begin{aligned} \tilde{V}_R(x, n\Delta s) &\cong \beta \sqrt{\Delta s \Delta y} \sum_{i=1}^m \sum_{j=1}^n \\ &\cdot G(x, i\Delta y; (n-j+1)\Delta s) N_{ij}, \quad n=1, 2, \dots, \end{aligned} \quad (5.27)$$

where N_{ij} , $i=1, 2, \dots, m$; $j=1, 2, \dots, n$ are independent standard normal random variables. The expected value of $\tilde{V}(x, n\Delta s)$ is given exactly by $\alpha[1 - \exp(-n\Delta s)]$ and is added to the values of \tilde{V}_R to obtain approximate sample paths for \tilde{V} . For small values of t , $G(x, y; t)$ is computed efficiently from the images representation

$$\begin{aligned} G(x, y; t) &= \frac{e^{-t}}{\sqrt{4\pi t}} \sum_{n=-\infty}^{\infty} \{ \exp[-(x-2nL-y)^2/4t] \\ &+ \exp[-(x-2nL+y)^2/4t] \}, \end{aligned} \quad (5.28)$$

whereas for large t an efficient computation is made from the eigenfunction expansion. Thus convergence difficulties are circumvented.

Examples

Both of the above simulation methods were carried out in order to estimate the moments and density of the interspike interval. In all the cases we report, the threshold condition is $\vartheta = 10$ at $x = 0$, the length of the nerve cylinder is $L = 1$, with sealed end conditions at $x = 0$ and $x = L$, and $\beta = 10$.

We first consider the case $\alpha = 30$. For the series simulation a time step of $\Delta s = 0.002$ was employed with 500 trials. With two terms in the Fourier series, the mean interspike time was $E[T] = 0.306$ (0.289, 0.323) where 95% confidence limits are indicated in brackets. When the stochastic integral was simulated with $\Delta s = 0.002$, $\Delta y = 0.05$ and 200 trials, the value of $E[T] = 0.262$ (0.240, 0.284). Thus there is a statistically significant difference in the mean interspike time obtained by the two methods.

For the smaller value of $\alpha = 10$, the series simulation with two terms, $\Delta s = 0.002$ and 500 trials gave $E[T] = 0.774$ (0.682, 0.807). The result by simulation of the stochastic integral with $\Delta s = 0.005$, $\Delta y = 0.05$ and 200 trials was $E[T] = 0.681$ (0.602, 0.759), so that there is no significant difference between the two results. For the series with 3 terms, the corresponding result was $E[T] = 0.654$ (0.603, 0.705) and the result obtained by solving the partial differential equation (5.16) by finite-differencing was $E[T] = 0.731$. The histogram of interspike times obtained by simulating two terms in the Fourier series is shown in Fig. 7.

The results obtained in the above examples represent very small interspike times. For physiological firing rates, values of $E[T]$ will usually be in the range 5–10 time constants, and possibly as great as 100 for spontaneously firing cortical cells (Burns and Webb, 1976). In such situations the first two terms in the Fourier series should give an adequate representation.

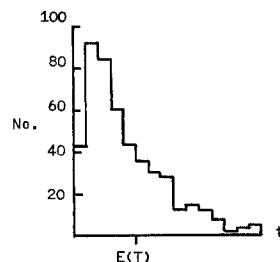


Fig. 7. Histogram of interspike intervals obtained by simulating the first two terms of the Fourier series representation of $\tilde{V}(x, t)$. For parameter values, see text

References

- Burns, B.D., Webb, A.C.: The spontaneous activity of neurones in the cat's cerebral cortex. *Proc. R. Soc. London B* **194**, 211–233 (1976)
- Conradi, S.: On motoneuron synaptology in adult cats. *Acta Physiol. Scand. Suppl.* **332**, (1969)
- Doob, J.L.: *Stochastic processes*. New York: Wiley 1953
- Dwight, H.B.: *Tables of integrals and other mathematical data*. New York: Macmillan 1961
- Dynkin, E.B.: *Markov processes*, Vol. II. Berlin, Heidelberg, New York: Springer 1965
- Finger, W., Stettmeier, H.: Efficacy of the two-electrode voltage clamp technique in crayfish muscle. *Pflügers Arch.* **387**, 133–141 (1980)
- Gradshteyn, I.S., Ryzhik, I.M.: *Tables of integrals, series, and products*. New York: Academic Press 1966
- Hodgkin, A.L., Huxley, A.F.: A quantitative description of membrane current and its application to conduction and excitation in nerve. *J. Physiol.* **117**, 500–544 (1952)
- Hodgkin, A.L., Rushton, W.A.H.: The electrical constants of a crustacean nerve fibre. *Proc. R. Soc. London B* **133**, 444–479 (1946)
- Holden, A.V., Yoda, M.: The effects of ionic channel density on neuronal function. *J. Theor. Neurobiol.* **1**, 60–81 (1981)
- Hooge, F.N.: $1/f$ noise. *Physica B* **83**, 14–23 (1976)
- Jack, J.J.B., Noble, D., Tsien, R.W.: *Electric current flow in excitable cells*. Oxford: Clarendon Press 1975
- Jack, J.J.B., Redman, S.J., Wong, K.: The components of synaptic potentials evoked in cat spinal motoneurons by impulses in single group Ia afferents. *J. Physiol.* **321**, 65–96 (1981)
- Koziol, J.A., Tuckwell, H.C.: Analysis and estimation of synaptic densities and their spatial variation on the motoneuron surface. *Brain Res.* **17**, 617–624 (1978)
- Matsumoto, G., Shimizu, H.: Spatial coherence and formation of collectively-coupled local nonlinear oscillators in squid giant axons. *J. Theor. Neurobiol.* **2**, 29–46 (1983)
- Rall, W.: Theory of physiological properties of dendrites. *Ann. N.Y. Acad. Sci.* **96**, 1071–1092 (1962)
- Rall, W.: Theoretical significance of dendritic trees for neuronal input-output relations. In: *Neural theory and modelling*. Reiss, R.F. (ed.). Stanford: Stanford University Press 1964
- Rall, W.: Core conductor theory and cable properties of neurons. In: *Handbook of physiology, Sect. 1. The nervous system. I. Cellular biology of neurons*. Kandel, E.R. (ed.). Am. Physiol. Soc. Bethesda (1977)
- Tuckwell, H.C., Wan, F.Y.M., Wong, Y.S.: The interspike interval of a cable model neuron with white noise input. *Biol. Cybern.* (in press, 1984)
- Walsh, J.B.: A stochastic model of neuronal response. *Adv. Appl. Prob.* **13**, 231–281 (1981)
- Walsh, J.B., Tuckwell, H.C.: Determination of the electrical potential over dendritic trees by mapping onto a nerve cylinder. I.A.M.S. Tech. Report. No. 83-8, Univ. of British Columbia, Vancouver 1983
- Wan, F.Y.M., Tuckwell, H.C.: The response of a spatially distributed neuron to white noise current injection. *Biol. Cybern.* **33**, 36–59 (1979)
- Wan, F.Y.M., Tuckwell, H.C.: Neuronal firing and input variability. *J. Theor. Neurobiol.* **1**, 197–218 (1982)

Received: July 11, 1983

Dr. Henry Tuckwell
Monash University
Department of Mathematics
Clayton, Victoria
Australia 3168